Detection of source granularity through multiparticle Bose correlations

W. N. Zhang, Y. M. Liu, L. Huo, and Y. Z. Jiang
Department of Physics, Harbin Institute of Technology, Harbin 150001, People's Republic of China

D. Keane
Department of Physics, Kent State University, Kent, Ohio 44242

S. Y. Fung
Department of Physics, University of California, Riverside, California 92521
(Received 14 June 1994; revised manuscript received 12 October 1994)

The multiparticle Bose correlations of bosons emitted from dispersed thermal droplets of quark-gluon plasma are simulated by a Monte Carlo method. Multiparticle Bose correlations can offer more sensitivity to probe the granularity of the boson-emitting source than two-particle Bose correlations. A promising signal of the existence of a mixed phase of quark-gluon plasma and hadronic gas can be obtained from multiparticle observables.

PACS number(s): 25.75.+r, 24.85.+p, 12.38.Mh

I. INTRODUCTION

The highest priority in ultrarelativistic heavy ion experiments is the detection of a new phase of nuclear matter, the quark-gluon plasma (QGP), and the study of its properties. There are reasons to expect that the phase transition predicted by QCD is a first-order phase transition [1–3]. A hallmark of this phase transition is the existence of a mixed phase of QGP and hadronic gas [3–6], and an important indicator of a QCD phase transition in ultrarelativistic heavy ion collisions would be the discovery of a particle-emitting source with a granular structure [4–6]. In the thermal droplet model [4], particles are emitted from dispersed thermal droplets of plasma, and the spatial distribution of the source is characterized by three parameters [5]: the thermal droplet radius a, the overall radius of the granular source R_0, and the mean separation d between the droplets. The number of droplets in the source, $n \sim (R_0/d)^3$, is also a useful parameter. Assuming that the distributions of droplets in the source and the locations of particle emission in a droplet both have Gaussian forms, the two-particle Bose correlation function is [5]

$$C_2^g(q) = 1 + \exp(-\tfrac{1}{2}q^2a^2)/n + \exp[-\tfrac{1}{2}q^2(a^2+R_0^2)](1-\tfrac{1}{n}), \quad (1)$$

where the superscript of $C_2^g(q)$ indicates the correlation function for a granular source, q is the relative momentum of the two particles, and the first and second exponential terms correspond to the cases of the two particles emitted from the same droplet and emitted from different droplets, respectively. Since the droplet radius a is much smaller than the radius of the granular source R_0, any enhancement of the correlation function in the large q region is mainly the result of correlations between two particles emitted from the same droplet, while correlations of two particles emitted from different droplets mainly affect the correlation function in the small q region. Pratt *et al.* [5] studied the two-tiered structure of the two-particle Bose correlation function for a granular source, and pointed out that positive kaons are the best candidate among the various kinds of bosons for the purpose of detecting and studying granularity. However, the two-particle Bose correlation function for a granular source may be difficult to distinguish from the two-particle Bose correlation function for a nongranular source which has a radius R between a and R_0; to make the distinction, we need excellent statistics and a thorough understanding of many effects associated with the physics of the interaction [7–12] and the resolution and acceptance of the detector [13] which complicate the interpretation. On the other hand, the high multiplicity of identical particles in ultrarelativistic heavy ion collisions provides the possibility of analyzing multiparticle correlations which may reveal very important information about the emitting source [8,14–20]. In this paper, the multiparticle Bose correlations of kaons emitted from dispersed thermal droplets are simulated by a Monte Carlo method and analyzed. We point out that granular and nongranular sources can be distinguished through studying and comparing the multiparticle Bose correlations in subevents with different multiplicities in an event, and information about the number of droplets in the emitting source can be inferred by analyzing pure multiplet Bose correlations.

II. MULTIPARTICLE CORRELATIONS IN A GRANULAR SOURCE

In the thermal droplet model, particles are emitted thermally and independently. A particle can be emitted from any one of the n droplets. If the ith boson is emitted from the point $\mathbf{r}_i'$ in the jth droplet, its spatial coordinate is

 ©1995 The American Physical Society

$$\mathbf{r}_i = \mathbf{R}_j + \mathbf{r}'_i\,, \quad i = 1,2,\ldots,M\,, \quad j \in \{1,2,\ldots,n\}\,, \tag{2}$$

where $\mathbf{R}_j$ is the central coordinate of the jth droplet, and M is the multiplicity of identical bosons. The probability of emitting M bosons of momenta $\mathbf{p}_1,\mathbf{p}_2,\ldots,\mathbf{p}_M \equiv \{\mathbf{p}\}$ from source points $\mathbf{r}_1,\mathbf{r}_2,\ldots,\mathbf{r}_M \equiv \{\mathbf{r}\}$ is

$$P(\{\mathbf{p}\};\{\mathbf{r}\}) \propto |\psi(\{\mathbf{p}\};\{\mathbf{r}\})|^2 g(\mathbf{p}_1,\mathbf{r}_1)\ldots g(\mathbf{p}_M,\mathbf{r}_M)\,, \tag{3}$$

where $g(\mathbf{p}_i,\mathbf{r}_i)$ is the probability of emitting a particle of momentum $\mathbf{p}_i$ from point $\mathbf{r}_i$. Neglecting the correlations of the spatial and momentum coordinates [5], $g(\mathbf{p}_i,\mathbf{r}_i)$ can be expressed as the product of the distribution of density $\rho(\mathbf{r}_i)$ and the single-particle-inclusive distribution of momentum $P(\mathbf{p}_i)$. In Eq. (3), $\psi(\{\mathbf{p}\};\{\mathbf{r}\})$ is the symmetrized final wave function of M identical particles, neglecting final state interactions [16,12],

$$\psi(\{\mathbf{p}\};\{\mathbf{r}\}) \propto \sum_\sigma \left[\prod_{j=1}^{M} \exp(i\mathbf{p}_j\cdot\mathbf{r}_{\sigma(j)})\right]\,, \tag{4}$$

where $\sigma(j)$ denotes the jth element of a permutation of the sequence $\{1,2,\ldots,M\}$, and $\sum_\sigma$ denotes the sum over all $M!$ permutations of this sequence. Integrating Eq. (3) over $\{\mathbf{r}\}$, one obtains $P(\{\mathbf{p}\})$, the probability to observe M final-state bosons of momenta $\{\mathbf{p}\}$ in an event.

Extending the two-particle correlation function of Pratt *et al.* [5] to the case of three-particle correlations, the three-particle correlation function for a granular source in the thermal droplet model can be expressed as

$$C_3^g(\mathbf{p}_1,\mathbf{p}_2,\mathbf{p}_3) = \frac{\int P_3(\mathbf{p}_1,\mathbf{p}_2,\mathbf{p}_3;\mathbf{r}_1,\mathbf{r}_2,\mathbf{r}_3)|\psi(\mathbf{p}_1,\mathbf{p}_2,\mathbf{p}_3;\mathbf{r}_1,\mathbf{r}_2,\mathbf{r}_3)|^2 d\mathbf{r}_1 d\mathbf{r}_2 d\mathbf{r}_3}{\int P_3(\mathbf{p}_1,\mathbf{p}_2,\mathbf{p}_3;\mathbf{r}_1,\mathbf{r}_2,\mathbf{r}_3) d\mathbf{r}_1 d\mathbf{r}_2 d\mathbf{r}_3}\,, \tag{5}$$

where

$$\begin{aligned}
P_3(\mathbf{p}_1,\mathbf{p}_2,\mathbf{p}_3;\mathbf{r}_1,\mathbf{r}_2,\mathbf{r}_3) &= g(\mathbf{p}_1,\mathbf{r}_1)g(\mathbf{p}_2,\mathbf{r}_2)g(\mathbf{p}_3,\mathbf{r}_3)\\
&= \sum_i^n\sum_j^n\sum_k^n \int d\mathbf{R}_i P(\mathbf{R}_i) d\mathbf{R}_j P(\mathbf{R}_j) d\mathbf{R}_k P(\mathbf{R}_k)[p(\mathbf{p}_1,\mathbf{r}_1-\mathbf{R}_i)p(\mathbf{p}_2,\mathbf{r}_2-\mathbf{R}_j)p(\mathbf{p}_3,\mathbf{r}_3-\mathbf{R}_k)]\\
&= \sum_i^n\sum_{j\neq i}^n\sum_{k\neq i,j}^n \int d\mathbf{R}_i P(\mathbf{R}_i) d\mathbf{R}_j P(\mathbf{R}_j) d\mathbf{R}_k P(\mathbf{R}_k)[p(\mathbf{p}_1,\mathbf{r}_1-\mathbf{R}_i)p(\mathbf{p}_2,\mathbf{r}_2-\mathbf{R}_j)p(\mathbf{p}_3,\mathbf{r}_3-\mathbf{R}_k)]\\
&\quad + \sum_i^n\sum_{j\neq i}^n \int d\mathbf{R}_i P(\mathbf{R}_i) d\mathbf{R}_j P(\mathbf{R}_j)[p(\mathbf{p}_1,\mathbf{r}_1-\mathbf{R}_i)p(\mathbf{p}_2,\mathbf{r}_2-\mathbf{R}_j)p(\mathbf{p}_3,\mathbf{r}_3-\mathbf{R}_j)\\
&\quad + p(\mathbf{p}_1,\mathbf{r}_1-\mathbf{R}_j)p(\mathbf{p}_2,\mathbf{r}_2-\mathbf{R}_i)p(\mathbf{p}_3,\mathbf{r}_3-\mathbf{R}_j) + p(\mathbf{p}_1,\mathbf{r}_1-\mathbf{R}_j)p(\mathbf{p}_2,\mathbf{r}_2-\mathbf{R}_j)p(\mathbf{p}_3,\mathbf{r}_3-\mathbf{R}_i)]\\
&\quad + \sum_i^n \int d\mathbf{R}_i P(\mathbf{R}_i)[p(\mathbf{p}_1,\mathbf{r}_1-\mathbf{R}_i)p(\mathbf{p}_2,\mathbf{r}_2-\mathbf{R}_i)p(\mathbf{p}_3,\mathbf{r}_3-\mathbf{R}_i)]\,,
\end{aligned} \tag{6}$$

where $P(\mathbf{R})$ is the normalized distribution of the centers of the droplets, and $p(\mathbf{p},\mathbf{r})$ describes the emission from an individual droplet about its center. Assuming $P(\mathbf{R}) \sim \exp(-|\mathbf{R}|^2/R_0^2)$, and $p(\mathbf{p},\mathbf{r}) \sim \exp(-|\mathbf{r}|^2/a^2)$ [5], it can be shown that

$$\begin{aligned}
C_3^g(\mathbf{p}_1,\mathbf{p}_2,\mathbf{p}_3) &= 1 + (1-\tfrac{1}{n})\{\exp[-\tfrac{1}{2}q_{12}^2(a^2+R_0^2)] + \exp[-\tfrac{1}{2}q_{13}^2(a^2+R_0^2)] + \exp[-\tfrac{1}{2}q_{23}^2(a^2+R_0^2)]\}\\
&\quad + \tfrac{1}{n}\{\exp(-\tfrac{1}{2}q_{12}^2a^2) + \exp(-\tfrac{1}{2}q_{13}^2a^2) + \exp(-\tfrac{1}{2}q_{23}^2a^2)\}\\
&\quad + \tfrac{2}{n^2}(n-1)(n-2)\{\exp[-\tfrac{1}{4}(q_{12}^2+q_{13}^2+q_{23}^2)(a^2+R_0^2)]\}\\
&\quad + \tfrac{2}{n^2}(n-1)\{\exp[-\tfrac{1}{4}(q_{12}^2+q_{13}^2+q_{23}^2)a^2 - \tfrac{1}{2}q_{12}^2R_0^2]\\
&\quad + \exp[-\tfrac{1}{4}(q_{12}^2+q_{13}^2+q_{23}^2)a^2 - \tfrac{1}{2}q_{13}^2R_0^2] + \exp[-\tfrac{1}{4}(q_{12}^2+q_{13}^2+q_{23}^2)a^2 - \tfrac{1}{2}q_{23}^2R_0^2]\}\\
&\quad + \tfrac{2}{n^2}\{\exp[-\tfrac{1}{4}(q_{12}^2+q_{13}^2+q_{23}^2)a^2]\}\,,
\end{aligned} \tag{7}$$

where $q_{ij} = |\mathbf{p}_i - \mathbf{p}_j|$. In Eq. (7), the second and third terms express the correlations of two particles emitted from different droplets and emitted from the same droplet, respectively; the fourth term expresses the pure triplet correlation of three particles emitted from different droplets; the fifth term expresses the pure triplet correlation of three particles where two are emitted from the same droplet and another emitted from a different droplet; and the sixth term expresses the pure triplet correlation for three particles emitted from the same droplet.

In order to analyze the three-particle correlation function and avoid complication caused by the number of variables, we consider the simpler symmetric configuration [21,22] $q_{12} = q_{13} = q_{23}$. The three-particle correlation function for a granular source reduces to

$$\begin{aligned}
C_3^g(q) &= 1 + 3(1-\tfrac{1}{n})\exp[-\tfrac{1}{2}q^2(a^2+R_0^2)] + \tfrac{3}{n}\exp(-\tfrac{1}{2}q^2a^2) + \tfrac{2}{n^2}(n-1)(n-2)\exp[-\tfrac{3}{4}q^2(a^2+R_0^2)]\\
&\quad + \tfrac{6}{n^2}(n-1)\exp[-\tfrac{3}{4}q^2a^2 - \tfrac{1}{2}q^2R_0^2] + \tfrac{2}{n^2}\exp(-\tfrac{3}{4}q^2a^2)\,.
\end{aligned} \tag{8}$$

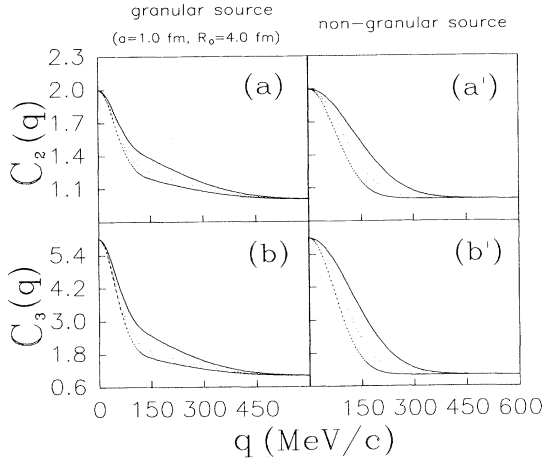

FIG. 1. Panels (a) and (a′) show two-particle correlation functions for a granular source and nongranular source, and (b) and (b′) show three-particle correlation functions in the case of a symmetric configuration for a granular source and nongranular source. The solid, dotted, and dashed lines in (a) and (b) correspond to $n = 2$, $n = 3$, and $n = 4$, respectively. The solid, dotted, and dashed lines in (a′) and (b′) correspond to $R = 1.5$ fm, $R = 2.0$ fm, and $R = 2.5$ fm, respectively.

In the case of a symmetric configuration, the three-particle correlation function for a nongranular Gaussian source with a radius R can be expressed as [8,16]

$$C_3^{ng}(q) = 1 + 3\exp(-\tfrac{1}{2}q^2R^2) + 2\exp(-\tfrac{3}{4}q^2a^2)\,. \quad (9)$$

Figure 1(a) shows the two-particle correlation function, Eq. (1), and Fig. 1(b) shows the three-particle correlation function, Eq. (8), in the case of a symmetric configuration for a granular source. We take $a = 1.0$ fm and $R_0 = 4.0$ fm [5] for the granular source. In Figs. 1(a) and 1(b), the solid, dotted, and dashed lines correspond to the number of droplets $n = 2$, $n = 3$, and $n = 4$, respectively. Figure 1(a′) shows the two-particle correlation function, $1+\exp(-q^2R^2/2)$, and Fig. 1(b′) shows the three-particle correlation function, Eq. (9), in the case of a symmetric configuration for a nongranular Gaussian source. In Figs. 1(a′) and 1(b′), the solid, dotted, and dashed lines correspond to nongranular source radii $R = 1.5$ fm, $R = 2.0$ fm, and $R = 2.5$ fm, respectively. From Fig. 1, it can be seen that the correlation functions for a granular source descend more rapidly with increasing q in the low q region, and converge towards unity more slowly in the high q region. Comparing the average correlation intensities over the region $0 < q < 600$ MeV/c in Fig. 1, the differences between granular and nongranular sources tend to be amplified when we use three-particle correlations in place of two-particle correlations. Furthermore, the average correlation intensities are stronger for the nongranular source than for the granular source in the low q region, while the opposite pattern is observed in the high q region. In particular, the average intensities show this characteristic more clearly for three-particle correlations than for two-particle correlations. These observations suggest that analyses of multiparticle correlations may offer advantages for distinguishing a granular source from a nongranular source with a radius between a and R_0.

The multiparticle correlation function for events with multiplicity M for a granular source is related to the number of droplets n and the multiplicity M, and involves many variables. Analytic treatments of such correlations are impractical, and it is customary to invoke Monte Carlo methods in multiparticle correlation analyses [8,16,19].

III. MONTE CARLO SIMULATIONS OF MULTIPARTICLE CORRELATION EVENTS IN THE THERMAL DROPLET MODEL

The Metropolis approach [23] is a standard Monte Carlo technique which allows one to generate an ensemble of multibody configurations according to a given probability density. Using this approach, Monte Carlo events with multiparticle correlations can be generated [16,19]. The procedure of our Monte Carlo simulations is as follows.

Step 1: generate the emission-point coordinates $\{\mathbf{r}\}$ of M particles from Eq. (2) according to the distribution of droplets in the source and the distribution of the emission points in a droplet, and generate the momenta $\{\mathbf{p}\}$ of M particles according to a given single-particle-inclusive distribution of momentum.

Step 2: generate $\mathbf{p}'_j$ ($j \in \{1,2,\ldots,M\}$) according to the single-particle-inclusive distribution of momentum, and calculate

$$w_{\rm old} = |\psi(\{\mathbf{r}\};\mathbf{p}_1,\ldots,\mathbf{p}_j,\ldots,\mathbf{p}_M)|^2\,,$$

$$w_{\rm new} = |\psi(\{\mathbf{r}\};\mathbf{p}_1,\ldots,\mathbf{p}'_j,\ldots,\mathbf{p}_M)|^2\,.$$

Step 3: accept the substitution of $\mathbf{p}'_j$ for $\mathbf{p}_j$ with the probability $\min(1, w_{\rm new}/w_{\rm old})$, and record $\{\mathbf{p}\}$.

Step 4: repeat steps 2 and 3 while incrementing j from 1 to M, and repeat N_1 times. A subset containing MN_1 correlated events for a certain $\{\mathbf{r}\}$ is generated.

Step 5: repeat steps 1 through 4 N_2 times, generating N_2 subsets of correlated events for different $\{\mathbf{r}\}$. The total number of correlated events is MN_1N_2.

In our calculations, both the distribution of droplets in the source and the distribution of the emission points in a droplet are of Gaussian form [5], the single-particle-inclusive distribution of momentum satisfies the Boltzmann distribution [4], and the temperature T is taken to be 180 MeV [2,17]. $|\psi(\{\mathbf{r}\};\{\mathbf{p}\})|^2$ is calculated using the Ryser-Wilf-Nijenhuis (RWN) algorithm [16,19,24]. Because of the requirement of ergodicity [23], the numbers N_1 and N_2 must be large enough. In the simulation of multiparticle correlated events, we require that the number of correlated events $MN_1 > 180$ for a given $\{\mathbf{r}\}$ and we require $N_2 > 40$.

Adapting the analyses of high-order collective flow correlations in Ref. [25], we use the following variable for analyzing the multiparticle Bose correlations:

$$Q_m = \left(\prod_{i<j\leq m}^{K} q_{ij} \right)^{1/K}, \quad m = 2, 3, \ldots, M,$$

$$K = m(m-1)/2, \tag{10}$$

where q_{ij} is the relative momentum of the ith and jth particles in a subevent of m particles selected randomly from an event, and the product runs over all K relative momenta formed from the subevent. The multiparticle correlation function is defined as

$$C(Q_m) = \mathrm{Cor}(Q_m)/\mathrm{Uncor}(Q_m), \tag{11}$$

where $\mathrm{Cor}(Q_m)$ is the distribution of Q_m obtained from the correlated events, and $\mathrm{Uncor}(Q_m)$ is the distribution of Q_m obtained from the events which do not contain any Bose correlations.

Figures 2(a), 2(b), and 2(c) show results for $C(Q_m)$ ($m = 2, 3, 4$), based on 7.2×10^3 Monte Carlo correlated events with multiplicity $M = 9$ for granular sources ($a = 1.0$ fm, $R_0 = 4.0$ fm). The open circle, open triangle, and open square symbols correspond to $n = 2$, $n = 3$, and $n = 4$, respectively; the corresponding results for nongranular sources ($n = 1$, $a = R$) are shown on the right, in Figs. 2(a'), 2(b'), and 2(c'), where the solid circle, solid triangle, and solid square symbols correspond to $R = 1.5$ fm, $R = 2.0$ fm, and $R = 2.5$ fm, respectively. From Fig. 2 it can be seen that the enhancement in $C(Q_m)$ increases with m, and the difference between the multiparticle correlation functions for granular and nongranular sources in comparison with the statistical errors increases with m also. Moreover, the number of combinations C_M^3 or C_M^4 sampling three or four particles from a multiparticle event ($M > 6$) is higher than the number of combinations C_M^2 sampling two particles. Thus, the multiparticle correlation functions in multiparticle events reflect the differences between granular and nongranular sources with better sensitivity than two-particle correlations.

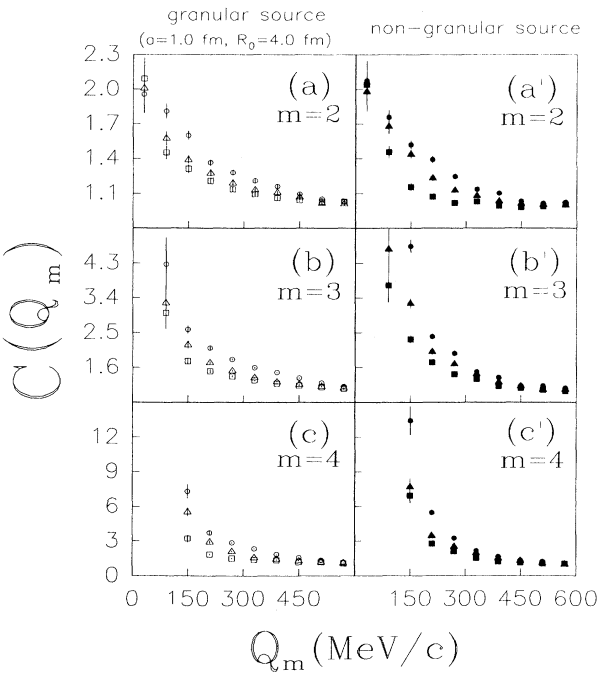

FIG. 2. $C(Q_m)$ of multiparticle events ($M = 9, m = 2-4$) for a granular source (a)–(c) and nongranular source (a')–(c'). The symbols ○, △, and □ in (a)–(c) represent $n = 2$, $n = 3$, and $n = 4$, respectively; the corresponding solid symbols in (a')–(c') represent $R = 1.5$ fm, $R = 2.0$ fm, and $R = 2.5$ fm, respectively.

IV. PROBING SOURCE GRANULARITY WITH MULTIPARTICLE CORRELATIONS

In order to elucidate the information contained in the multiparticle correlation functions $C(Q_m)$ in Fig. 2, we define

$$S_m = \frac{1}{N_{\mathrm{bin}}} \left[\sum_{Q_m^{(1)} \leq Q_m \leq Q_m^{(2)}} C(Q_m) \right], \tag{12}$$

where N_{bin} is the number of bins used over the interval $[Q_m^{(1)}, Q_m^{(2)}]$, and the sum denotes the sum of the values of $C(Q_m)$ in those bins.

Figures 3(a) and (a') show the values of S_m for multiparticle events ($M = 9$) with granular and nongranular sources, respectively, calculated for the multiparticle correlation functions $C(Q_m)$ plotted in Fig. 2. Since the statistics for the multiparticle correlation functions obtained from the region $Q_m < 120$ MeV/c are poor, we study the Q_m region between 120 MeV/c and 600 MeV/c. In Figs. 3(a) and 3(a'), the open square, solid circle, and open triangle symbols correspond to $m = 2$, $m = 3$, and $m = 4$, respectively. Comparing Figs. 3(a) and 3(a'), it can be seen that although the value of S_2 for the granular source with a given number n of droplets may be close to a value of S_2 for a nongranular source with some radius $R = R'$ between a and R_0, the value of S_m for the granular source with the given n becomes smaller than the value of S_m for the nongranular source with radius R' when m increases. The probability of emitting m particles from the same droplet decreases rapidly, and the probability of emitting m particles from different droplets increases with increasing m. Furthermore, when the values of S_2 for both kinds of source are close to each other, the radius R' of the nongranular source is smaller than the radius R_0 of the granular source, and the average correlation between particles emitted from different droplets in the granular source is much weaker than the average correlation between the particles emitted from the nongranular source. Thus, by comparing the values of S_m for different m, including the pattern of increase of S_m with m, we can distinguish a granular source from a nongranular source. The correlation among particles emitted from different droplets mainly affects the multiparticle correlation function for a granular source in the small Q_m region. The multiparticle

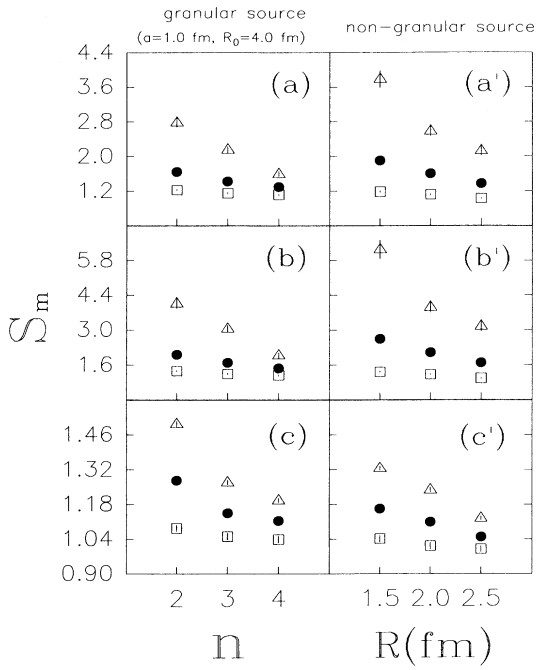

FIG. 3. S_m results for a granular source (a)–(c) and nongranular source (a′)–(c′) for multiparticle events ($M = 9$); (a) and (a′) for $Q_m^{(1)} = 120$ MeV/c, $Q_m^{(2)} = 600$ MeV/c, (b) and (b′) for $Q_m^{(1)} = 120$ MeV/c, $Q_m^{(2)} = 360$ MeV/c, (c) and (c′) for $Q_m^{(1)} = 360$ MeV/c, $Q_m^{(2)} = 600$ MeV/c. The symbols □, •, and △ correspond to $m = 2$, $m = 3$, and $m = 4$, respectively.

correlation function for a granular source in the large Q_m region gets its main contribution from the correlation among particles emitted from the same droplet, which is stronger than the correlation between particles emitted from a nongranular source with radius R between a and R_0. Therefore, the differences between the multiparticle correlation functions of a granular source and a nongranular source with radius R between a and R_0 in the small and large Q_m regions may be different. Figures 3(b) and 3(c) show the granular source results for S_m in the small Q_m region (between 120 and 360 MeV/c) and in the large Q_m region (between 360 and 600 MeV/c), respectively, based on multiparticle events with multiplicity $M = 9$. Again, Figs. 3(b′) and 3(c′) show the corresponding results for the nongranular source, and we have used the same values of m and the same symbols as in Figs. 3(a) and (a′). It can be seen from Figs. 3(b) and 3(b′) that in the small Q_m region, the S_3, and S_4 results for granular sources corresponding to $n = 2$, 3, and 4 are smaller than the S_3 and S_4 results for nongranular sources corresponding to $R = 1.5$ fm, 2.0 fm, and 2.5 fm, respectively. These, in turn, are opposite to the results in Figs. 3(c) and 3(c′) for the large Q_m region. This is a promising signal for distinguishing granular and nongranular sources, and we conclude that S_m is an important observable to probe the granularity of the source.

V. THE NUMBER OF DROPLETS IN THE EMITTING SOURCE

From Eq. (1), it is clear that the effect of source granularity on the two-particle correlation functions in two-particle events is related to the number of droplets n. In multiparticle events, the effect of source granularity on multiparticle correlation functions is not only related to n, but also related to the multiplicity M of identical bosons. We define the average number of bosons emitted from a droplet as

$$\langle N \rangle = M/n . \tag{13}$$

When $\langle N \rangle$ becomes larger, the effect of source granularity on multiparticle correlation functions becomes stronger.

Because the radius R_0 of a granular source is much larger than the radius of a droplet, the correlations between the particles emitted from different droplets are much weaker than the correlations between the particles emitted from the same droplet, especially in the large Q_m region, and the contribution of the correlations between the particles emitted from different droplets to the multiparticle correlation function can be neglected. Therefore, in the large Q_m region, there will not be a contribution from pure m-multiplet correlations in the multiparticle correlation function, as long as $\langle N \rangle < m$. When $\langle N \rangle > m$, the sample of correlated particles will contain m particles emitted from the same droplet, and the multiparticle correlation function will contain contributions from pure m-multiplet correlations. We define

$$F_m = S_m - S_{m-1} ; \tag{14}$$

compared with S_m, F_m gives additional prominence to the contribution of the pure m-multiplet correlations in the m-particle correlation function. Figure 4 gives results for F_3 (solid circle symbol), F_4 (open triangle symbol), and F_5 (open circle symbol) for multiparticle events with a granular source ($a = 1.0$ fm, $R_0 = 4.0$ fm) in the Q_m region between 300 and 600 MeV/c. Figures 4(a), 4(b), and 4(c) show results for events with multiplicities $M = 6$, $M = 9$, and $M = 12$, respectively. In Fig. 4(a), when n increases from 2 to 3, the value of $\langle N \rangle$ decreases from 3 to 2, and F_3 is also seen to decrease. Since $\langle N \rangle$ is always smaller than 4 in this case (for $n = 2, 3, 4$), there is no contribution from pure quadruplet correlations in S_4, and the increments of S_3 to S_4 and S_2 to S_3 only contain contributions from triplet and pair correlations; accordingly, F_3 and F_4 almost overlap. In Fig. 4(b), when $n = 2$ and $\langle N \rangle = 4.5$, F_4 is higher than F_3, while there is not much difference between F_5 and F_4; when $n = 3, 4$, $\langle N \rangle < 4$, and F_4 decreases from its value at $n = 2$ while F_5, F_4, and F_3 almost overlap since there are no contributions from pure quintuplet and quadruplet correlations. In Fig. 4(c), when $n = 2$, $\langle N \rangle > 5$ and there are differences both between F_5 and F_4 and between F_4 and F_3 because of contributions from pure quintuplet and quadruplet correlations. When $n = 3$, F_5 and F_4 begin to overlap, and likewise when $n = 4$, F_4 and F_3 begin to overlap. Therefore, by analyzing the contributions of pure multiplet correlations in multipar-

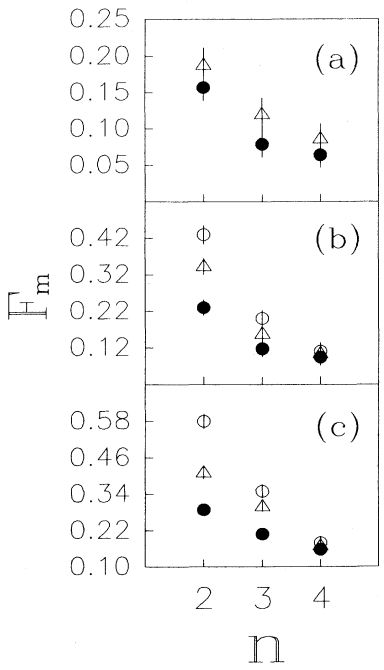

FIG. 4. F_m results for multiparticle events with a granular source in the Q_m region between 300 and 600 MeV/c; (a) for $M = 6$, (b) for $M = 9$, and (c) for $M = 12$. The symbols •, △, and ○ correspond to $m = 3$, $m = 4$, and $m = 5$, respectively.

ticle correlation functions, we can determine the average number $\langle N \rangle$ of bosons emitted from a droplet. If F_m and F_{m-1} begin to overlap as the multiplicity m of the subevent increases to m_0, then there are no contributions from pure m-multiplet correlations in S_m, and it can be inferred that the average number of bosons $\langle N \rangle$ emitted from a droplet lies between $(m_0 - 1)$ and m_0. In that case, information about the number of droplets in the emitting source can be inferred from Eq. (13).

Final-state Coulomb interactions for kaons can be neglected in the present context. Coulomb repulsion between charged kaons mainly affects particles with relative momentum smaller than $(m_K \alpha^{1/2})$ ~42 MeV/c [7,26], but is much less important at the higher relative momenta where spatial structures with dimensions of 5 fm or less are probed. In our simulations, the number of correlated kaon pairs below 42 MeV/c in relative momentum is very low — only about 0.04% of all correlated kaon pairs. Results with a cut $q_{ij} \geq (m_K \alpha^{1/2})$ in the region $Q_m \geq$120 MeV/c are indistinguishable from results without the cut, so the influence of final-state Coulomb interactions on analyses of source granularity with the expected dimensions can be neglected.

If the source lifetime is not negligibly short, averaging over all directions of relative momentum $\mathbf{q}$ might obscure information about the source granularity contained in the two-particle correlation function. However, two-particle correlations among the components of relative momentum transverse to their total momentum is not affected by the source lifetime [3,26,5]. By choosing particles with the same magnitude of momentum so that each pair among the analyzed particles has its relative momentum perpendicular to the total momentum of the pair, any smearing resulting from the finite source lifetime can be circumvented.

VI. CONCLUSIONS

Interferometry analyses for identical bosons produced in ultrarelativistic heavy ion collisions is an important tool to probe possible granularity in the spatial structure of the source and so shed light on the existence of the phase of quark-gluon plasma [5,6,27]. Because of limited statistics and the many complex factors that can influence the interpretation of interferometry measurements, probing the granularity of the emission source using only two-particle Bose correlation may be very difficult. Compared to two-particle Bose correlations, multiparticle Bose correlations can reflect the difference between granular and nongranular sources with better sensitivity. Granular sources can be detected by comparing and analyzing the multiparticle Bose correlations in subevents with different multiplicities in different relative momentum regions, and a possible signal of the existence of a mixed phase of QGP and hadronic gas can be sought. In multiparticle events, the effect of source granularity on multiparticle Bose correlation functions relates to the average number of bosons $\langle N \rangle$ emitted from a droplet, and contributions from pure m-multiplet correlations in multiparticle correlation functions in the large relative momentum region for the cases of $\langle N \rangle > m$ and $\langle N \rangle < m$ show distinct differences. This can be used to determine the average number of bosons emitted from a droplet by analyzing the pure multiplet Bose correlations in the large relative momentum region. Pratt *et al.* [5] have enumerated several advantages of kaons for detecting source granularity through interferometry, including copious emission, less distortion arising from the decay of long-lived resonances, and well-understood final state interactions. We argue that multikaon correlations may offer a promising signal to probe the QCD phase transition.

ACKNOWLEDGMENTS

This work is supported by the National Natural Science Foundation of China, the U.S. Department of Energy, and the U.S. National Science Foundation.

[1] M. Gyulassy, K. Kajantie, H. Kurki-Suonio, and L. McLerran, Nucl. Phys. **B237**, 477 (1984).
[2] J. B. Kogut and D. K. Sinclair, Phys. Rev. Lett. **60**, 1250 (1988).
[3] S. Pratt, Phys. Rev. D **33**, 1314 (1986).
[4] D. Seibert, Phys. Rev. Lett. **63**, 136 (1989).
[5] S. Pratt, P. J. Siemens, and A. P. Vischer, Phys. Rev. Lett. **68**, 1109 (1992).
[6] T. Kajino, Phys. Rev. Lett. **66**, 125 (1991).
[7] M. Gyulassy, S. K. Kauffmann, and L. W. Wilson, Phys. Rev. C **20**, 2267 (1979).
[8] Y. M. Liu, D. Beavis, S. Y. Chu, S. Y. Fung, D. Keane, G. VanDalen, and M. Vient, Phys. Rev. C **34**, 1667 (1986).
[9] M. G. Bowler, Z. Phys. C **39**, 81 (1988).
[10] S. S. Padula and M. Gyulassy, Phys. Lett. B **217**, 181 (1989).
[11] M. Gyulassy and S. S. Padula, Phys. Rev. C **41**, R21 (1989).
[12] S. S. Padula, M. Gyulassy, and S. Gavin, Nucl. Phys. **B329**, 357 (1990); *ibid.* **B339**, 378 (1990).
[13] For example, see "Conceptual Design Report for the Solenoidal Tracker at RHIC," The STAR Collaboration, Report No. PUB-5347, 1992.
[14] Y. M. Liu, D. Beavis, S. Y. Chu, S. Y. Fung, D. Keane, G. VanDalen, and M. Vient, in *Proceedings of International Symposium on Medium Energy Physics*, Beijing, 1987, edited by H. C. Chang and L. S. Zhen (World Scientific, Singapore, 1987), p. 557.
[15] W. Willis and C. Chasman, Nucl. Phys. **A418**, 425c (1984).
[16] W. A. Zajc, Phys. Rev. D **35**, 3396 (1987).
[17] J. G. Cramer, Phys. Rev. C **43**, 2798 (1991).
[18] N. Neumeister *et al.*, Phys. Lett. B **275**, 186 (1992).
[19] W. N. Zhang, Y. M. Liu, S. Wang, Q. J. Liu, J. Jiang, D. Keane, Y. Shao, S. Y. Fung, and S. Y. Chu, Phys. Rev. C **47**, 795 (1993); Y. M. Liu, W. N. Zhang, S. Wang, Y. Z. Jiang, D. Keane, S. Y. Fung, and S. Y. Chu, High Energy Phys. Nucl. Phys. **14**, 281 (1990); W. N. Zhang, Y. Z. Jiang, S. Wang, Y. M. Liu, D. Keane, J. Jiang, Y. Shao, S. Y. Fung, and S. Y. Chu, *ibid.* **16**, 439 (1992).
[20] S. Pratt, Phys. Lett. B **301**, 159 (1993).
[21] M. Biyajima, A. Bartl, T. Mizoguchi, N. Suzuki, and O. Terazawa, Prog. Theor. Phys. **84**, 931 (1990).
[22] M. Plumer, L. V. Razumov, and R. M. Weiner, Phys. Lett. B **286**, 335 (1992).
[23] N. Metropolis, A. W. Rosenbluth, M. N. Rosenbluth, A. H. Teller, and E. Teller, J. Chem. Phys. **21**, 1087 (1953).
[24] A. Nijenhuis and H. S. Wilf, *Combinatorial Algorithms*, 2nd ed. (Academic, New York, 1978).
[25] J. Jiang, D. Beavis, S. Y. Chu, G. Fai, S. Y. Fung, Y. Z. Jiang, D. Keane, Q. J. Liu, Y. M. Liu, Y. Shao, M. Vient, and S. Wang, Phys. Rev. Lett. **68**, 2739 (1992).
[26] S. Pratt, Phys. Rev. D **33**, 72 (1986).
[27] G. F. Bertsch, Nucl. Phys. **A498**, 173c (1989).